ISSN 2348-313X (Print)
International Journal of Life Sciences Research ISSN 2348-3148 (online)
Vol. 7, Issue 2, pp: (518-530), Month: April - June 2019, Available at: www.researchpublish.com

Core shell quantum dots induced apoptosis in human hepatocellular carcinoma cells *via* Reactive oxygen species-mediated mitochondrial-dependent pathway

Aakriti Tyagi[1], Namrata Kumari[1], Ankita Leekha[1], Disha Mittal[1], Anita Kamra Verma*

[1]*Corresponding author: Anita Kamra Verma, Nanobiotech Lab, K.M.College, University of Delhi. Delhi.

*Email: akverma@kmc.du.ac.in.

Abstract: **This study addresses the current knowledge of Quantum Dots (QDs) as drugs, targeting probes and as drug delivery carriers. We proposed to evaluate the toxic effects of oleic acid capped inverted core/shell QDs against Human hepatocellular carcinoma cell line-Hep3B. We investigated two types of core/shell QDs with identical nature of their shell (CdSe) and different core (ZnSe-*vs*-CdS), the other properties affecting cellular responses– capping, particle size, shell and surface chemistry were kept constant. IC_{50} of QDs on Hep3B cells was achieved at 10µg/ml within 24 h. Incubation for 72 h with ZnSe/CdSe QDs produced an insignificant reduction in cell viability (63.44%). Hence the cellular responses were evaluated at the maximum concentration i.e 10µg/ml. LDH release enhanced on treatment with ZnSe/CdSe (45.64µM/min/mgprotein) and CdS/CdSe (39.49µM/min/mgprotein) when compared to untreated control (9.38µM/min/mgprotein). Enhanced DCFDA levels indicated ROS generation on treatment with QDs. ROS induced ER stress leading to increased release of intracellular calcium levels were observed. Disruption of MMP caused enhanced cytochrome-c levels that induced caspase-dependent cascade. Elevated apoptotic events were observed as evidenced by enhanced expression of apoptotic proteins, caspases and DNA fragmentation. These findings suggest that QDs have the potential for biological applications. Therefore, the toxicological risk of QDs need be assessed before embarking on any clinical use.**

Keywords: **Hepatocellular carcinoma, QDs, ROS, ER Stress, mitochondrial membrane potential, Caspase cascade, apoptotic pathway.**

I. INTRODUCTION

Hepatocellular carcinoma (HCC), also called malignant hepatoma, is the most common type of liver cancer and occurs predominantly in patients with underlying chronic liver disease and cirrhosis. The threat of HCC is expected to continue to grow in the coming years. [El-Serag HB, Rudolph KL 2007]. Chemotherapy is the first line of treatment for all cancers. However, one of the major obstacles to successful chemotherapy has been the toxicity of chemotherapeutic drugs to normal cells and tissues. Apparently, there is an imperative need to identify new therapeutic agents for the treatment of HCC.

Nanotechnology is a growing field in industry that leads to a broad range of nanomaterials suitable for biomedical applications. This advanced field manipulates and creates materials at nanoscale levels to produce nanoproducts with novel properties. In recent times, quantum dots (QDs), nanotubes, fullerene derivatives and nanowires have gained massive attention in developing novel kinds of analytical tools for medical sciences [Bruchez et al., 1998], [Taton et al., 2000], [Cui et al., 2001]. However, the pharmacological and toxicological effects of these novel materials have not been reported.

QDs also termed as nanoscale semiconductor crystals, are the type of nanoparticles with characterstic electronic and optical properties like bright and intensive fluorescence [Matea C.T et al 2017]. They are with a narrow size distribution and high luminescent efficiency which has generated interest in various researchers due to their wide applications in area of biological fluorescence labeling and medical research [Chen T et al 2013].

In comparison with the II–VI group QDs, such as CdSe and CdTe QDs, ZnO QDs are cheap and have biocompatibility with biological systems [Xiong, Xu, Ren, 2008], [Xia, 2008] that has lead to great interest in biological labelling and photocatalytic applications. Also, the anticancer activity of CdSe QDs against MCF-7 cell line with the induction of ROS has been suggested. [Sanwalni et al 2014]. Bhanoth et al (2015) also reported the cytotoxic effects of hydrobic QDs CdS/CdSe against MCF-7 and EAC.

Therefore we have assessed the cytotoxic effects of ZnSe/CdSe and CdS/CdSe against Hepatocellular Carcinoma (Hep3B) cells by MTT assay, which may lead to DNA fragmentation and apoptosis by the induction of ROS generation. Membrane permeability and the changes in the Mitochondrial Membrane potential was also analysed by LDH and Rhodamine-123, respectively.

II. MATERIALS AND METHODS

A. Chemicals

(3-(4,5-dimethyathiazol-2-yl)-2,5-diphenyltetrazolium bromide (MTT), Dimethyl sulphoxide (DMSO), Sodium bicarbonate, Bovine Serum Albumin (BSA), HEPES (Hydroxy ethyl piperazineethanesulphonic acid), Ribonuclease A, DCFH-DA (2',7'-dichlorofluorescin diacetate), DHE (dihydroethidium), DAPI (4´,6-diamidino-2-phenylindole), Fluo-3/AM, and Rhodamine 123 were procured from Sigma-Aldrich Chemical Co., USA. The growth medium DMEM (Dulbecco's Minimum Essential Media) and fetal bovine serum (FBS) were supplied by Gibco BRL. Trypsin was supplied by Himedia, India. Tris HCl, Trichloroacetic acid (TCA), Triton® X-100, Ethylene diamine tetra-acetic acid (EDTA), DPA (Diphenylamine), Sodium dodecyl sulphate (SDS), Phenol, chloroform, isoamyl alcohol**,** agarose, ethidium bromide were supplied by SRL, India. Proteinase K was procured from Roche, Mannheim, Germany. Bax, bcl_2, Caspase3, Caspase 9, and Cytochrome C monoclonal antibody, FITC conjugated secondary antibody (anti-mouse for Bax (cat# 610982) and Bcl-2 (cat# 51-6511GR) in 1:200 dilution) [rabbit polyclonal antibody for Caspase-9 p10 (H-83: sc-7885), Caspase-3 (H-277: sc-7148), and NFkBp65 (H-268: sc-7151) were supplied by BD Biosciences. Human Hepatocellular Carcinoma-Hep3B, HepG2 cell lines and Human Embryonic Kidney cell line-HEK293 were ordered from National Centre for Cell Sciences (NCCS), Pune. All the chemicals procured were of analytical grade and used without further purification.

B. Cell culture

Hep3B, HepG2 and HEK-293 cell lines were maintained in DMEM supplemented with 10% FBS. *In vitro*, Cells were grown in a humidified atmosphere of 5% CO_2 at 37ºC in CO_2 incubator (Thermo Scientific, USA). For trypsinization, the 80-90% confluent culture flask was treated with 0.01% trypsin-EDTA in PBS pH-7.4 and the reaction was stopped by adding few drops of FBS and further the trypsinized cells was washed twice by complete DMEM medium. For the cryo-preservation the trypsinized cells ($4x10^6$) were resuspended in 1ml of freezing medium (90% FBS and 10% DMSO mixture) and stored at liquid nitrogen.

C. Cytotoxicity Assay

The degree of mitochondrial reduction of the tetrazolium salt (MTT) was measured spectrophotometrically to evaluate mitochondrial function. Biotoxicity of QDs was measured by the MTT assay (tetrazolium method) [Verma et al 2014]. In a 96 well microplate, exponentially growing cells were inoculated at density 5 x 10^3 cells/well in 100 µl FBS supplemented DMEM. Cells were treated with three concentrations of QDs (2.5µg/ml, 5µg/ml and 10µg/ml). Cells were incubated with QDs for two time points (24h and 48h) and later on 20 µl MTT (5 mg/ml) was added to each well followed by incubation at 37ºC. The media was carefully pipette out after 4h without disturbing the cells and for dissolving the formazan crystals 150 µl DMSO was added to each well. After 10 minutes the absorbance were measured at 540 nm by a UV spectrometer. The cytotoxicity was calculated and by plotting the drug concentration versus the % cytotoxicity of QDs [Verma, A.K *et al*. 2005].

D. Cellular Uptake by Fluorescence Microscopy and time dependent kinetic study

Healthy, growing Hep3B cells were inoculated on 12mm round glass cover slip at $5x10^4$ cells per well in a 24 well microplate with 500µl of 10% FBS supplemented DMEM [Verma et al 2014]. Hep3B cells were treated with core/shell quantum dots for 3 hours and to remove uninternalized particles washed twice with PBS. The cells were fixed and permeabilized with 4% paraformaldehyde and 0.2% Triton X-100 respectively. After permeabilization, DAPI (1µg/ml) was added to the treated cells. After placing a cover slip over the cells, the slides were mounted in DPX and were visualized by fluorescent upright microscope under bright field, blue filter and red filter (Nikon Eclipse 90i)).

To perform kinetic study, the medium of Hep3B cells grown to a confluence of 80%–90% in a 24 well plate was replaced with a fresh serum free medium followed by treatment with QDs (10µg/mL) in triplicates. At different intervals, PBS was used (three times) to wash and remove the QDs from the cell surface. Treated cells with PBS were then analyzed using a spectrophotometer (Infinite M200 PRO multimode microplate readers- TECAN, Männedorf, Switzerland).

E. LDH release assay

To prepare samples for the LDH assay, cells are passaged and cells were seeded at a density of 5×10^3 cells/well (DMEM containing 10% FBS) grown for 24 hr before QDs exposure. The cells were dosed with different concentrations of QDs in DMEM medium containing 1% FBS. After 24 hr exposure, the 96-well plates were shaken briefly to homogenize the released LDH in the cell culture medium and the medium was transferred to 1.5 ml microcentrifuge tubes and were centrifuged at 12,000g at 4 °C for 15 min to remove any cell debris and unbound QDs. 100µl of each sample was added to the substrate solution (30 mM sodium pyruvate) and then added 6.6 mM NADH and the absorbance at 340 nm was measured using a spectrophotometer (TECAN, Switzerland). The LDH activity of the samples was obtained by measuring the decreasing rate of NADH absorbance over time.

F. ROS assay by fluorescent microscopy and fluorometry

Hep3B cells treated with QDs at 10µg/ml for 24 h were incubated with a fluorogenic dye, DCFH-DA, that examine cellular reactive oxygen species (ROS) activity within the cell for 30 min at 37°C in dark. After incubation, cells were washed with PBS and immediately the mean green fluorescence of cells was quantified in spectrofluorimeter (Agilent Technologies, U.S.A).

A qualitative analysis of ROS generation 24 h exposure of QDs was done using fluorescent microscopy. Hep3B cells were cultured in 24 well culture plates over cover slips till 90% confluence was attained and treated with QDs for 24 h at concentration of 10µg/ml. The treated cells were harvested, washed with PBS and followed by incubation for 30 min in dark with DCFH-DA at 37°C. Incubation with fluorogenic dye is followed by PBS wash and fixation with 4% paraformaldehyde, DPX mounting and visualization by fluorescent upright microscope (Nikon Eclipse 90i) at 20x under bright field and FITC filter.

G. Intracellular calcium levels [Ca^{2+}]i

In a 96-well plate, exponentially growing Hep3B cells were seeded as per procedure followed for the MTT assay. Subsequent day, after changing the media of the cells, they were treated with different concentrations of QDs (2.5 to 10µg/ml) for 24 h. Incubated cells were washed twice with PBS and were loaded with 5 mM Fluo-3/AM for 30 min in the dark at 37 °C followed by another wash with PBS to remove excess Fluo-3/AM. To observe the affect, fluorescent intensity (485 nm excitation and 520 nm emission) was recorded in a Synergy HT multimode microplate reader. A percentage increase in fluorescence intensity with respect to controls was used to express the intracellular [Ca^{2+}] variations.

Mitochondrial Membrane Potential (MMP)

Rhodamine 123, a fluorescent probe, is used to monitor the mitochondrial membrane potential (MMP) as an index to determine mitochondrial dysfunction in treated cells. Briefly, in a 24-well plate, Hep3B cells were seeded at density of 5×10^4 cells/ml per well. The following day, cells were treated with QDs at 10µg/ml concentration for 24 h. After incubation, treated cells were washed thrice with serum-free DMEM medium and incubated with 50nM Rhodamine 123 for 30 min in dark at 37°C. Finally, incubated cells were washed with PBS and spectrophotometrically analyzed to measure the mitochondrial membrane potential at excitation wavelength of 488 nm and emission at 530nm by using fluorescent micro-plate reader (TECAN, Switzerland). Slides were prepared by incubating Hep3B cells with QDs at 10µg/ml concentration

for 24 h in a 24-well plate at density of 2×10^4 cells/ml/well. Treated cells were incubated with Rhodamine 123 for 30 min in dark at 37°C. The cells were collected and washed twice with PBS followed by fixation in 4% paraformaldehyde. Fixed cells were immediately analyzed under fluorescent microscope using FITC filter at 20X magnification.

H. Immuno-cytochemistry

Exponentially growing hepatocellular carcinoma cell lines, Hep3B, were seeded in a 24 well cell culture plates on 12mm round glass cover slip. 70-80% confluent cells were treated with core shell QDs at 10µg/ml concentration for 24 hours. Treated cells were washed thrice with PBS and fixed in 4% paraformaldehyde for 5 minutes at room temperature. 0.1% Triton-X in PBS was used to permeabilized these fixed cells followed by washing the cells with PBS. The cells were later incubated with bax, bcl2, Cyt. C caspase-9, caspase-3 and NFkB monoclonal antibody and were placed overnight at 4°C. The following day, to the incubated cells FITC conjugated secondary antibody (anti-mouse for Bax (cat# 610982) and Bcl-2 (cat# 51-6511GR) in 1:200 dilution) [rabbit polyclonal antibody for caspase-9 p10 (H-83: sc-7885), caspase-3 (H-277: sc-7148) and NFkBp65 (H-268: sc-7151) (BD biosciences) was added followed by another step of incubation at room temperature for 2 hrs [Tramu, G., et al., 1978]. Finally, the cells were washed with PBS and by using DPX mountant carefully mounted on glass slides and visualized in the fluorescent microscope (Nikon Eclipse 90i).

I. DPA (Diphenylamine) assay for DNA fragmentation

Hep3B cells were treated with QDs at 10µg/ml concentration for 24 hours and were resuspended in 800µl of PBS and 700µl of ice-cold lysis buffer containing 0.5% (v/v) Triton X-100, 20mM ethylenediaminetetraacetic acid (EDTA) and 5mM Tris-HCl. Lysate were incubated on ice for 15 minutes and then to separate fragmented DNA from high molecular weight DNA lysates were centrifused at 13,000g for 15 min at 4°C. The supernatant containing degraded DNA was transferred to new tubes and the pellet containing intact DNA was resuspended in 1500µl of TE buffer (10mM Tris, pH 8.0 and 1mM EDTA pH 8.0). 1500µl of 10% TCA were added to each tube and further incubated at room temperature for 10 min. After incubation, centrifuged and resuspended the pellet in 700µl 5% TCA, the mixture was boiled for 10-15 minutes, cool to room temperature and centrifuged again. 500 µl of supernatant was transferred to new tubes and incubated with 1ml diphenylamine reagent overnight at 30°C. The following day, absorbance was measured at 600nm and the percentage of DNA fragmentation was calculated [Gercel-Taylor C. et al 2005].

Percentage of DNA fragmentation= $O.D_{600}$ of the supernatant/ [$O.D_{600}$ of the supernatant+ $O.D_{600}$ of the pellet]* 100.

J. Statistical Analysis

The results were expressed as mean ± SD (n=3). One-way ANOVA was used to analyse the comparison among groups and Tukey's test using Prism (5.0) software (Prism software Inc. CA) was used to separate means. Levels of significance were accepted at ≤0.05 level.

III. RESULTS AND DISCUSSION

We assessed the potential of oleic acid capped inverted core/shell QDs, ZnSe/CdSe and CdS/CdSe, in causing toxicity against Hepatocellular carcinoma (HCC). Previously, our group reported synthesis of these QDs [Sreenu et al 2014], [Sreenu et al 2015], [Sreenu et al 2016a], [Sreenu et al 2016b], [Sreenu et al 2016 c] and anti-cancer activity against non-cancerous HEK-293 and breast cancer cell line MCF-7. Selenium-N heterocyclic compound cyclohexeno-1, 2, 3-selenadiazole, an organometallic, was used as the selenium precursor while cadmium precursor was cadmium acetate. The particles were capped with oleic acid as capping agent. The core/shell QDs were spherical in morphology and approximately 3nm-4nm in size. CdSe on the surface of the ZnSe/CdSe, and CdS/CdSe nanoparticles acts as a shield between QDs and the surroundings. The capping possibly slows the oxidative process in the cell responsible for the non-specific toxicity. This enhanced the protection of the QD core by the surface modification, controls the release of Cd^{2+} ions into the cytoplasm.

The HEK cells were less susceptible to QDs in which only 29%, 46.1% and 51%, and killing was reported at 2.5µg/ml, 5 µg/ml and 10 µg/ml and concentrations respectively, while higher susceptibility of HepG2 cell lines to QDs with 79.4%, 63.4% and 63% observed cytotoxicity within 48h (Fig). Hep3B and HepG2 were selected as an *in vitro* Hepatocellular Carcinoma models. Hep3B, Hepatocellular carcinoma cells were more susceptible to QDs as evident by IC_{50} observed after 24 h treatment with ZnSe/CdSe and CdS/CdSe, respectively (Fig.1). All the core/shell QDs showed concentration and time dependence cytotoxicity. In QDs treated Hep3B cells, 50% inhibition of cell growth were achieved even at

ISSN 2348-313X (Print)
International Journal of Life Sciences Research ISSN 2348-3148 (online)
Vol. 7, Issue 2, pp: (518-530), Month: April - June 2019, Available at: www.researchpublish.com

10µg/ml, maximum tested dose within 24 h. In subsequent experiments to evaluate the cellular responses, the maximum concentration was used in Hep3B cell line.

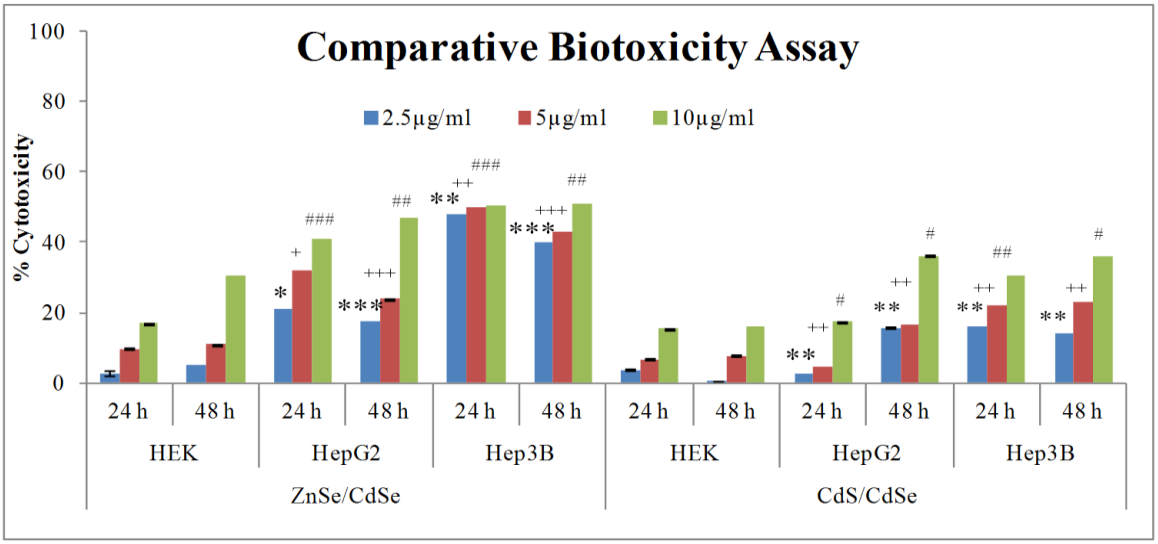

Fig 1: Assessement of cytotoxicity at different time interval in different concentration

* denotes significant difference between control HEK *vs* HepG2 and Hep3B of ZnSe/CdSe conc. 2.5µg/ml;
+ denotes significant difference between control HEK *vs* HepG2 and Hep3B of ZnSe/CdSe conc. 5µg/ml;
# denotes significant difference between control HEK *vs* HepG2 and Hep3B of ZnSe/CdSe conc. 10µg/ml;
*p<0.05; **p<0.01; p<0.001

Cellular uptake

To assess the internalization of core shell quantum dots, cellular uptake was performed. Hep3B cells were incubated with quantum dots for 2h followed by fixation and were analyzed by fluorescence microscopy at a magnification of 20x. The fluorescemce intensity of cells in Fig 2 indicated that core/shell ZnSe/CdSe and CdS/ CdSe were unifromly internalized within the cells. In both the cases, we found that our QDs were internalized in a simillar way by the cells as they share similar size and surface chemistry (same CdSe shell and capping with oleic acid) and localized predominanently in the cytoplasm and in the perinuclear regions of the cells.

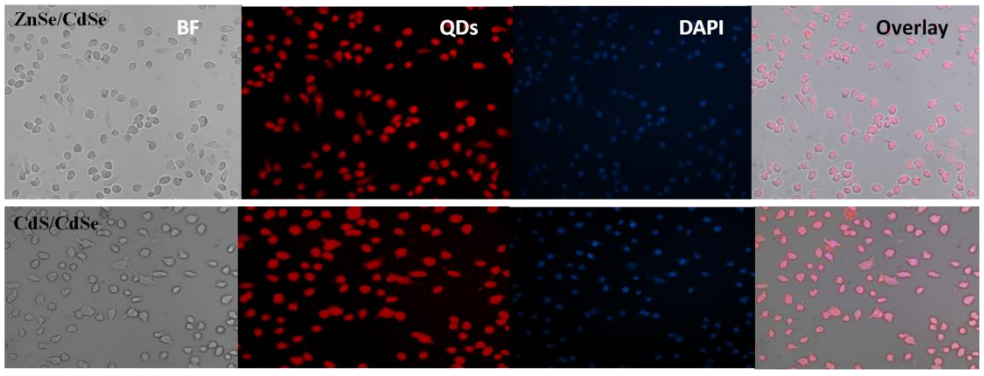

Fig 2: Intracellular localization of ZnSe/CdSe and CdS/CdSe with Hep3B cells observed under fluorescent microscope (Mag. 20x).

Time dependence of cellular uptake of QDs

Differential cellular uptake efficiencies of different QDs by Hep3B cells were investigated. In the present study, we detected fluorescent intensity of core shell quantum dots in Hep3B cells, which include the total fluorescent intensity of fluorescence from endosomes/lysosomes and cytoplasm and not the differential fluorescence between them. As shown in fig. 3, the increasing rate of QDs uptake over initial time points was faster. The uptake rates of QDs have reached the

ISSN 2348-313X (Print)
International Journal of Life Sciences Research ISSN 2348-3148 (online)
Vol. 7, Issue 2, pp: (518-530), Month: April - June 2019, Available at: www.researchpublish.com

equilibrium after incubation with QDs for 2 hrs in Hep3B cells, which indicated that the binding at the cellular surface has also reached the saturation (fig. 3). It is reported that the non specific binding would be expected due to ionic interactions. The increasing rate of QDs uptake over initial time points was higher, and the final uptake efficiency were much less in the cells.

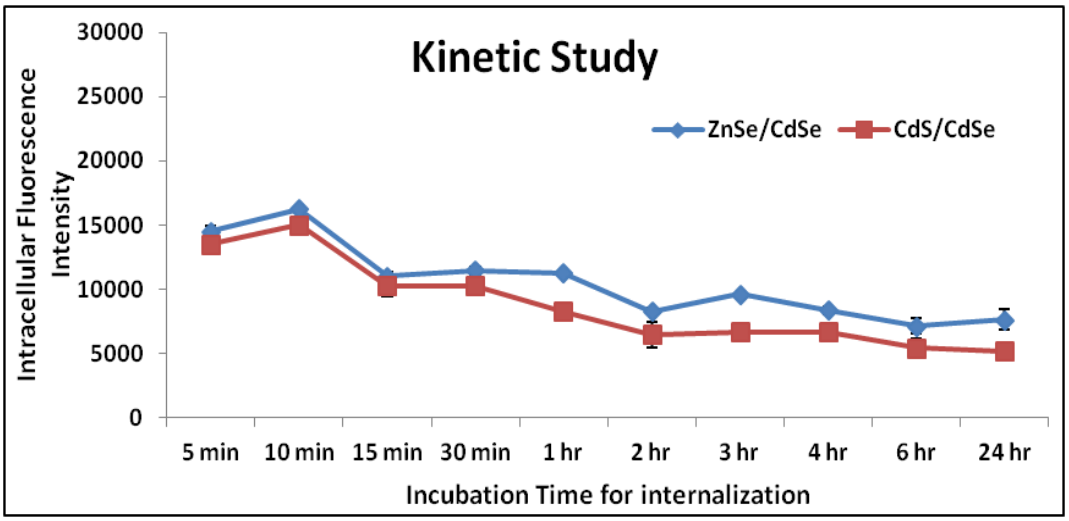

Fig. 3: Graph indicating the intracellular localization of ZnSe/CdSe and CdS/CdSe (10µg/ml) with Hep3B cells cell lines.

Lactate dehydrogenase (LDH) release/membrane integrity

In order to assess the cellular integrity, LDH (lactate dehydrogenase) membrane leakage assay was performed. The cells were exposed to QDs at 2.5µg/ml, 5µg/ml and 10µg/ml for 24 h. The observed results indicated that indeed treatment with core/shell QDs: ZnSe/CdSe and CdS/CdSe induced significant membrane damage in Hep3B cells in dose dependent manner. ZnSe/CdSe showed significantly enhanced LDH release (45.64µM/min/mg protein) at 10µg/ml as compared to CdS/CdSe (39.49µM/min/mg protein) and untreated control cells (9.38µM/min/mg protein) (Fig.4).

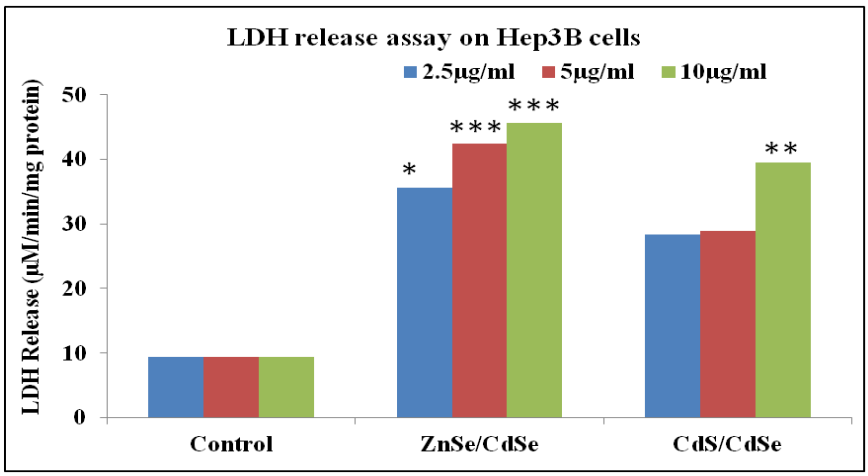

Fig 4: Assessment of cellular integrity by LDH release assay post 24 h treatment with ZnSe/CdSe and CdS/CdSe at three different concentrations: 10µg/ml, 5µg/ml and 2.5µg/ml QDs for 24 h.

* denotes significant difference between untreated control cells and ZnSe/CdSe treated cells and between untreated control cells and CdS/CdSe treated cells.

*p<0.05; **p<0.01; p<0.001

Reactive Oxygen Species (ROS) estimation

In every normal cell, a subtle balance is maintained between formation of free radicals and their removal. However, this balance may shift towards the side of free radical formation when antioxidant levels are depreciated. When this buffering capacity of cells gets attenuated attributing to physiological insults resulting in excess of ROS, this occurrence of state of

ISSN 2348-313X (Print)
International Journal of Life Sciences Research ISSN 2348-3148 (online)
Vol. 7, Issue 2, pp: (518-530), Month: April - June 2019, Available at: www.researchpublish.com

imbalance is termed as "oxidative stress" [Bertonici, C.R and Meneghini, R., 1995]. Oxidative stress may also result in severe damage to DNA, proteins and lipids, thereby, altering the structure and function of organism. Prolonged stress may play a critical role in progression of certain degenerative and chronic diseases, including cardiovascular disease, autoimmune disease, cancer, etc. [Roberts, J.A. and Hubel, C.A., 2004].

Quantitative and Qualitative analysis of intracellular ROS

DCFH-DA directly measures the redox state of a cell and has been used for the detection of Peroxynitrite ($ONOO^-$), hydrogen peroxide (H_2O_2) and hydroxyl radicals ($OH^·$) mediated oxidation in the cells and intacellular ROS production. H_2O_2 is not a free radical thus its reactivity is much lower than other free radicals generated during ROS production. We investigated the qualitative data by fluorescence microscopy. Photographs (Fig. 5I) clearly represent the production of intracellular ROS by DCFH-DA dye in Hep3B cells. DCF reacts with hydroxyl radical (OH.) and form fluorescent compound. As a result for quantitative analysis by fluorimeter for ROS shows increase in fluorescent intensity (Mag-20x).

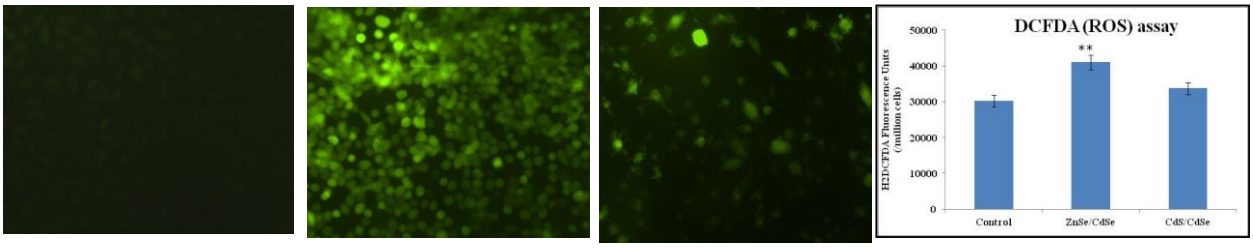

(I) (A) Control (B) ZnSe/CdSe (C) CdS/CdSe (II)

Fig 5: (I) Photographs showing the qualitative estimation of intracellular ROS generation using DCFH-DA dye in Hep3B cells *via* fluorescent microscopy. (a) Control, (b) ZnSe/CdSe and (c) CdS/CdSe treated Hep3B cells at 10µg/ml for 24 h. (II) Quantitative estimation of ROS generation by QDs stimulation in Hep3B cells by DCFDA assay *via* fluorescent spectrophotometer.

* denotes significant difference between untreated control cells and ZnSe/CdSe treated cells and between untreated control cells and CdS/CdSe treated cells.

*p<0.05; **p<0.01; p<0.001

DNA Damage

It is well known that oxidative stress is produced in cells by oxygen-derived species resulting from cellular metabolism and from interaction with cells of exogenous sources such as carcinogenic compounds, redox-cycling drugs and ionizing radiations. DNA damage caused by oxygen-derived species including free radicals is the most frequent type encountered by aerobic cells, and it is called oxidative DNA damage that can produce a multiplicity of modifications in DNA including base and sugar lesions, strand breaks, DNA-protein cross-links and base-free sites. In our experiment, DNA cleavage under control conditions was around 10.6% and was quantified using the diphenylamine (DPA) assay. Hep3B cells treated with 10µg/ml of ZnSe/CdSe and CdS/CdSe for 24 h significantly enhanced the DNA fragmentation to 55%, and 42% respectively (fig 6).

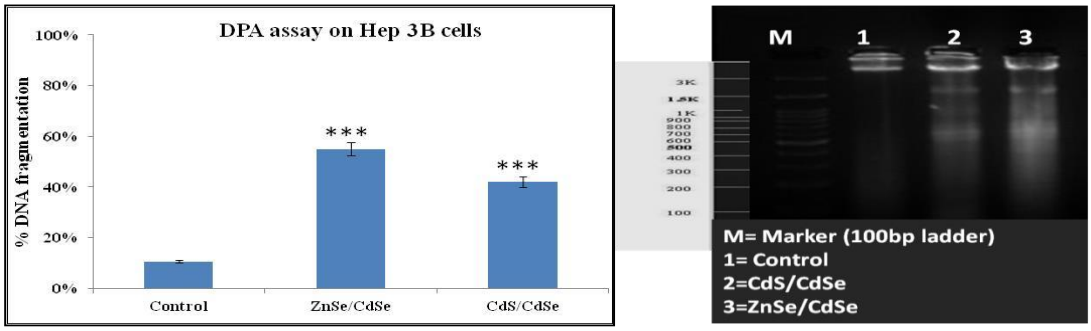

(A) (B)

Fig 6: (A) Quantification of DNA fragmentation of Hep3B cells using DPA assay in the control and experimental groups. Bar are mean ± S.D. Values in the parenthesis are percent change from that of control. (B) Quantification of DNA fragmentation of Hep3B cells *via* agarose gel electrophoresis. Lane M: Marker (3K-100bp), Lane 1: Untreated Hep3B cell's DNA sample; Lane 2: CdS/CdSe treated Hep3B cell's DNA sample; Lane 3: ZnSe/CdSe treated Hep3B cell's DNA sample.

ISSN 2348-313X (Print)
International Journal of Life Sciences Research ISSN 2348-3148 (online)
Vol. 7, Issue 2, pp: (518-530), Month: April - June 2019, Available at: www.researchpublish.com

* denotes significant difference between untreated control cells and ZnSe/CdSe treated cells and between untreated control cells and CdS/CdSe treated cells.

*p<0.05; **p<0.01; p<0.001

Measurement of intracellular Ca^{2+} levels

Intracellular Ca^{2+} levels were measured with 4mM Fluo-3/AM staining by both fluorescent microscopy and by fluorometry. As shown in Fig. 7(1) treatments of Hep3B cells with QDs at 10µg/ml for 24 h increased the fluorescence when compared with the control. ZnSe/CdSe (128.86±7.81%) displayed a higher increase in the fluorescence intensity in comparison to CdS/CdSe (110.28±6.24%) at same dose (10µg/ml) (fig 7(2)).

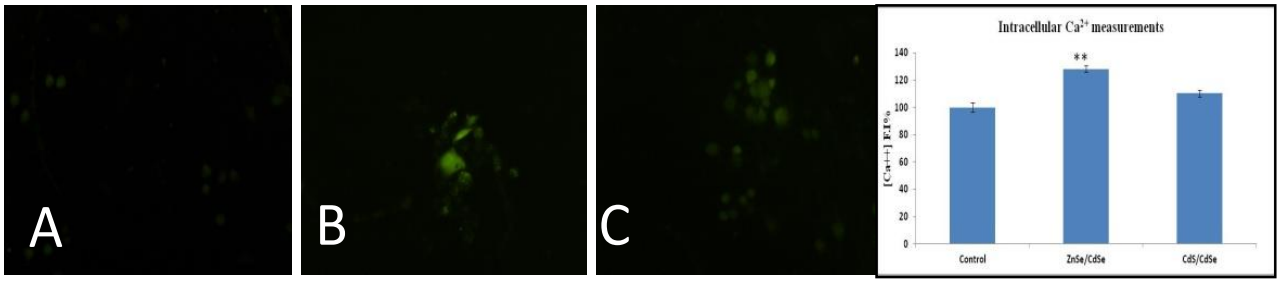

Fig 7: Effects of QDs on the increase of intracellular Ca^{2+} in Hep3B cells. Cells were treated with QDs at 10µg/ml.(1) Intracellular Ca^{2+} was measured by fluorescence microscopy and (2) Fluorometry analysis. The data were presented as mean ± SD (*n* = 3). Fluorometry (FLUO3-AM: excitation wavelength, 506 nm; emission wavelength, 526 nm, monitored at FL-1 channel).

All values are presented as mean ± S.D. (n ≥3). * denotes significant difference between untreated control cells and ZnSe/CdSe treated cells and between untreated control cells and CdS/CdSe treated cells.
*p<0.05; **p<0.01; p<0.001

QDs-induced loss of MMP in Hep3B cells

Mitochondrial Membrane Potential was measured using the modified method of Pourahmad et al. 2003. The uptake of the Rhodamine 123, a cationic Fluorescent dye, was used for the estimation of the mitochondrial membrane potential [Andersson et al., 1987]. To evaluate the occurrence of alterations in MMP on treatment of Hep3B cells with QDs at concentration of 10µg/ml for 24 h, analysis was carried out and the fluorescence intensity of Rhodamine 123 was measured. Fig 8(I) indicated ZnSe/CdSe showed more disruption of MMP at the concentrations of 10µg/ml for 24 h displayed a noteworthy disruption of MMP as compared to the control of CdS/CdSe as ZnSe/CdSe shows43.65% intensity as compared to CdS/CdSe thatshowed 53.37% only (fig.8II).

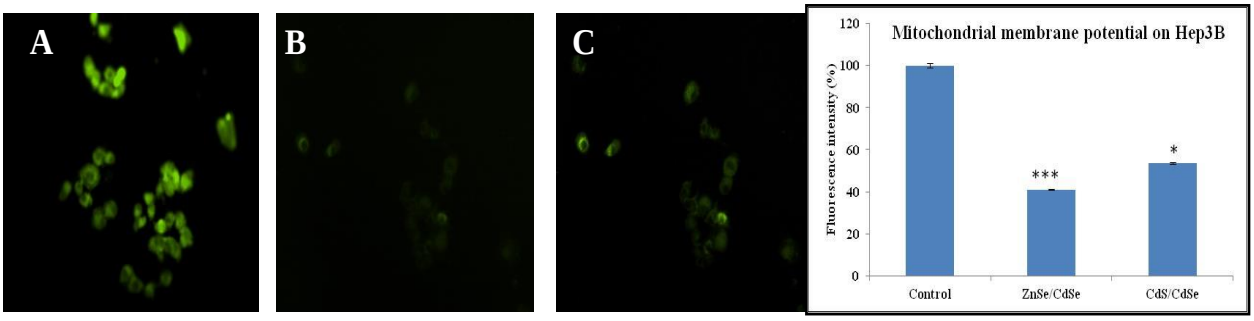

Fig 8: Effects of QDs on integrity of mitochondrial membrane in Hep3B cells. (I) MMP was measured by fluorescence microscopy (20X) and (II) Fluorometry analysis. The data were presented as mean ± SD (*n* = 3). Fluorometry (Rhodamine 123: excitation wavelength, 488 nm; emission wavelength, 530 nm, monitored at FL-1 channel).

ISSN 2348-313X (Print)
International Journal of Life Sciences Research ISSN 2348-3148 (online)
Vol. 7, Issue 2, pp: (518-530), Month: April - June 2019, Available at: www.researchpublish.com

All values are presented as mean ± S.D. (n ≥3). * denotes significant difference between untreated control cells and ZnSe/CdSe treated cells and between untreated control cells and CdS/CdSe treated cells.
*p<0.05; **p<0.01; p<0.001

Elucidation of the Molecular mechanism

In vitro Immunocytochemical Staining Analysis of Differential Expression of Bax, Bcl-2, Cytochrome C, Caspase-9, Caspase-3, NFkB in Hepatocellular carcinoma-Hep3B cell line

To study the molecular mechanism involved in the toxicity induced by QDs, Bax, Bcl-2 and caspase-3 and -9 along with cytochrome C and NFkB were detected by immunocytochemistry.

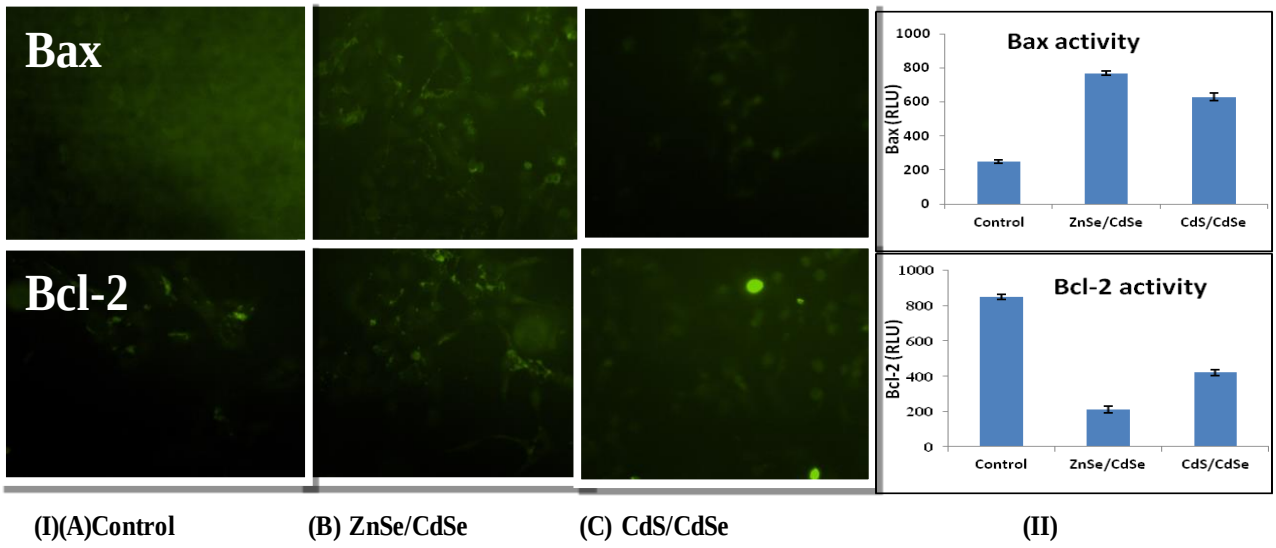

Fig. 9: Relative luminescence expression (RLU) of Bax and Bcl-2 in Hep3B cells by immunocytochemistry after 24 hr post treatment with ZnSe/CdSe and CdS/CdSe.(I) Observed under fluorescent Microscope (20X) (II) Expression Profile. Untreated Hep3B cells served as control. Maximum expression of Bax was observed in when Hep3B cell line was treated with ZnSe/CdSe.

In the control group, Bax and Bcl-2 had different levels of expression. The CdS/CdSe treated cells were largely identical to the control group and the staining was relatively lighter than ZnSe/CdSe treated cells. In the ZnSe/CdSe treated cells there was significantly enhanced Bax expression while Bcl-2 expression was low as compared to control while in CdS/CdSe the expression of Bax was low as compared to ZnSe/CdSe treated cells while Bcl-2 expression higher. The ratio of Bax/Bcl-2 appeared to increase with ZnSe/CdSe > CdS/CdSe (fig.9 I, II).

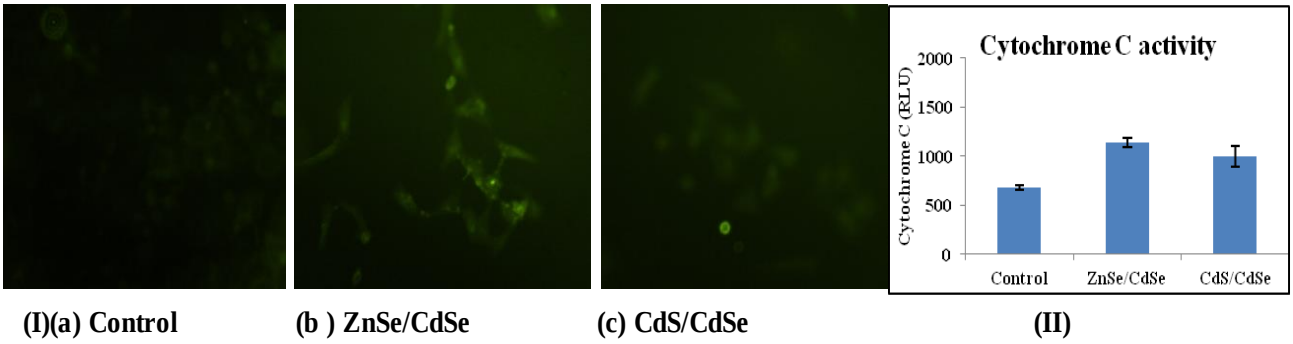

Fig. 10: Relative luminescence expression (RLU) of Cytochrome C in Hep3B cells by immunocytochemistry after 24 hr post treatment with ZnSe/CdSe and CdS/CdSe. (I) Observed under Fluoroscent Microscope (20X). (II) Expression Profie.

The expression of Cyt. C was significantly enhanced in ZnSe/CdSe treated cells as compared to CdS/CdSe. Untreated cells showed basal expression of Cyt C. Release of Cyt. C from mitochondria to cytosol is a key step in the execution of the cell death pathway i.e. apoptosis (fig.10).

ISSN 2348-313X (Print)
International Journal of Life Sciences Research ISSN 2348-3148 (online)
Vol. 7, Issue 2, pp: (518-530), Month: April - June 2019, Available at: www.researchpublish.com

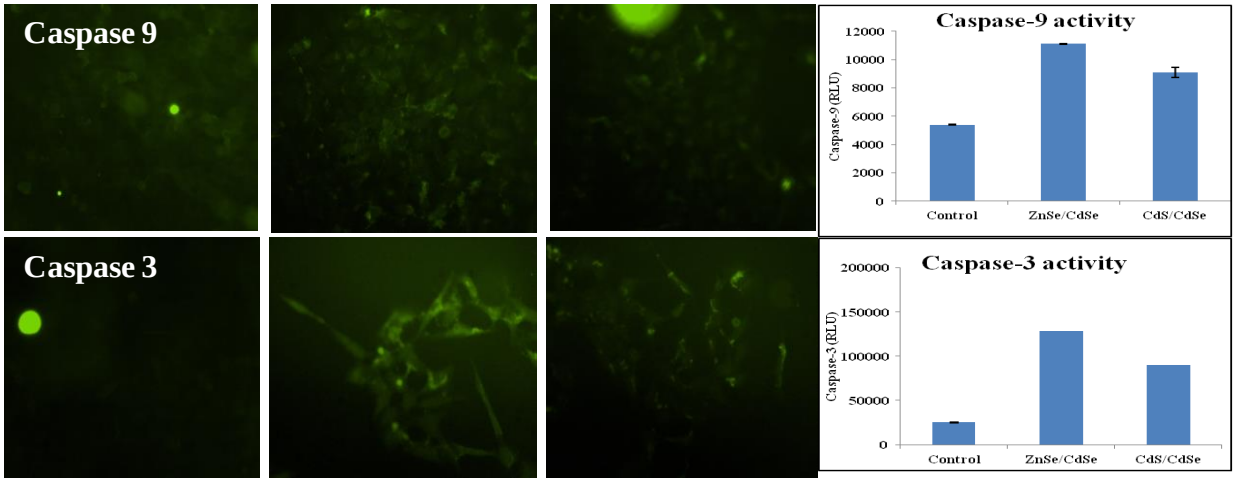

(I)(a) Control **(b) ZnSe/CdSe** **(c) CdS/CdSe** **(II)**

Fig 11: Relative luminescence expression (RLU) of caspase-9 and caspase-3 in Hep3B cells by immunocytochemistry after 24 hr post treatment with ZnSe/CdSe and CdS/CdSe. Untreated Hep3B cells served as control.(I) Observed Under Microscope (20X). (II) Expression Profile. Maximum expression of caspase-9 and -3 was observed in when Hep3B cell line was treated with ZnSe/CdSe.

He, N. et al, 2013 and Fulda, S. et al 2010 stated that mitochondria is the major pathway for apoptosis and thus by targeting it is a novel strategy for cancer therapy. Caspases play a major role among the death proteases and belongs to a family of aspartate-directed cysteine-dependent proteases. Caspases are of two types, that is initiator or upstream caspases and effector or downstream caspases. In an induced caspase dependent pathway initiator caspases, namely caspase-8 and caspase-9 activates effector caspases which includes caspase-3 and caspase-7; by cleaving their inactive pro-forms. The active forms of effector caspases further cleave proteins which participate in programmed cell death process. Increased activity of caspase-3 and caspase-9 was observed in Hep3B cells on treatment with core shell QDs as compared to untreated cells. Maximum caspase-3 activity (1,28,142 RLU) was achieved by ZnSe/CdSe treatment at concentration of 10µg/ml. The untreated controls only expressed caspase activity (fig.11). Similarly, caspase-9 activity was also elevated on treatment with QDs. All the QDs showed caspase-9 activity of more than 9,000 RLU. When the caspase-9 activity of control cells was just 5,400 RLU, while the highest activity was showed by ZnSe/CdSe at concentrations of 10µg/ml was 11,108 RLU followed by CdS/CdSe with 9,102 RLU**.** On the whole, QDs showed increase in caspase-9 dependent caspase-3 activity suggesting that there is an activation of both intrinsic and extrinsic apoptotic pathways.

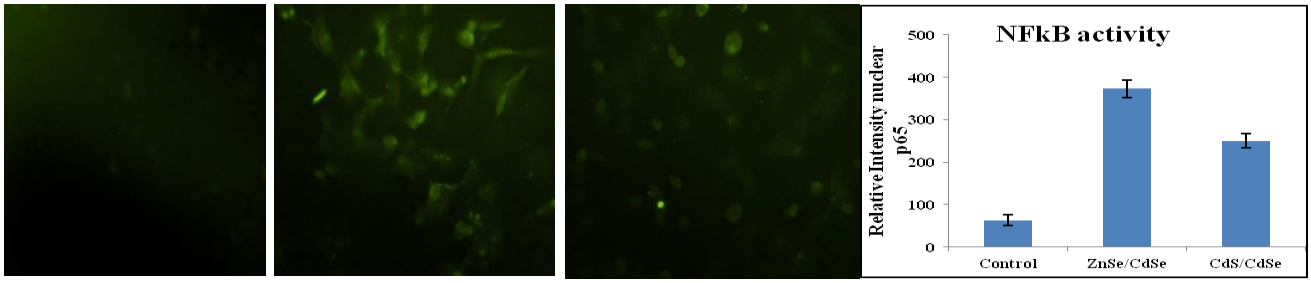

(I) (a) Control **(b) ZnSe/CdSe** **(c) CdS/CdSe** **(II)**

Fig 12: Immunocytochemistry and Relative luminescence expression (RLU) of NFkB in Hep3B cells by immunocytochemistry after 24 hr post treatment with ZnSe/CdSe and CdS/CdSe. (I)Observed Under Fluoroscent Microscope (20X). (II) Expression Profile.

Oxidative stress is a defence mechanism, but over the time it increases protein damage, lipids and DNA. The activation of the transcription factor NF-kB, a critical immediate early response gene to injury, can be another way to cause apoptosis, QDs interestingly induced activation of the NF-kB pathway due to the oxidative stress. NF-kB is an important upstream regulator of various cytokines induced in response to diverse stimuli as well as ROS. QDs also increased the cytosolic Ca^{2+} concentration that may cause activation of NF-kB. Increase of intracellular calcium can cause further increase in production of reactive oxygen species through signalling cascade that induces a positive feedback

ISSN 2348-313X (Print)
International Journal of Life Sciences Research ISSN 2348-3148 (online)
Vol. 7, Issue 2, pp: (518-530), Month: April - June 2019, Available at: www.researchpublish.com

mechanism. Green fluorescence represents cells stained with p65 subunit antibody of NF-kB after treatment with QDs. ZnSe/CdSe induced a strong NF-kB nuclear translocation, 373 RLU, as compared to control (63 RLU) (fig.12). After CdS/CdSe exposure, significant nuclear translocation was observed with 250 RLU of fluorescent cells after 24 h exposure. Fig 12 shows enlarged view of NF-kB localization from cytosol to nuclei. Maximum expression of NFkB was observed in when Hep3B cell line treated with ZnSe/CdSe QDs.

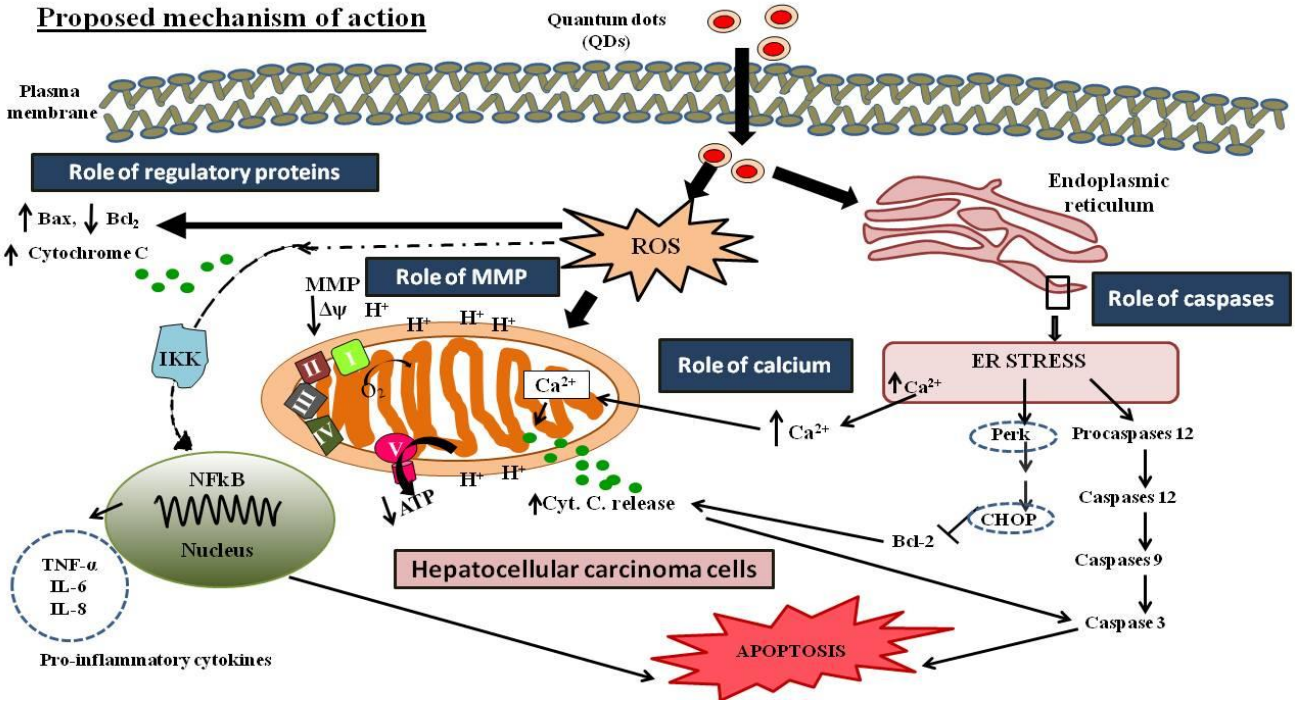

Fig. 13: Proposed possible mechanism of action of core/shell quantum dots

From the results we have proposed a mechanism of action of QDs. Similarly QDs increased the ROS production and Ca^{2+} concentration in cytoplasm of Hep3B cells, the intracellular accumulation of ROS and Ca^{2+} further induced the loss of MMP. The disruption of MMP caused release of Cyt C from mitochondria to cytosol. Cytosolic Cyt C activated the pro-caspase-9 and subsequently, caspase-9 activated the downstream effector caspases-3, Cyt C eventually triggered apoptosis of Hep3B cells**.** Therefore, QDs induced ROS generation and disruption of MMP leads to the release of Cyt C followed by the induction of pro-apoptotic factors, such as Bax. ZnSe/CdSe induces more expression of Cyt C, upregulation of Bax, down regulation of Bcl-2 as compared to CdS/ CdSe. Therefore ZnSe/CdSe causes enhanced apoptosis as compared to CdS/CdSe in Hep3B cells.

We have demonstrated that our core/shell QDs induced ROS and in turn triggered ER stress. ZnSe/CdSe treatment increased the sensitivity of Hep3B cells to ER stress in comparison to CdS/CdSe. Also, our results showed that toxicity mechanisms of QDs is characterised by ROS production, ER stress and release of Ca^{2+} from ER, translocation of Bax to mitochondria, depolarisation of MMP and activation of caspase 9 and caspase 3. Interestingly, leakage of Ca^{2+} from ER stress induces mitochondrial damage and ROS production. Cytoplasmic calcium concentration relies on the influx of Ca^{2+} through the plasma membrane and through channels of the ER while concentration in mitochondria depends on the cytoplamsic concentration. A rise in cytoplasmic Ca^{2+} concentration is coupled with enhanced mitochondrial Ca^{2+} concentration and eventually results in impaired MMP. Apoptotic cross talk between mitochondria and ER is based on the calcium signalling, leakage of calcium from ER and uptake of cytoplamic calcium into mitochondria, which is activated by Bax while constrained by Bcl-2 [Kim et al 2008], [Bhandary B et al 2009], [Bhandary B et al 2012], [Verfaillie T et al 2013], [Moin I et al 2018]. Thus, our data showed that ROS induces ER stress and rise in calcium leakage from ER to cytoplasm, over-expression of Bax, reduced expression of Bcl-2, mitochondrial fission, release of cytochrome c, precipitating apoptosis, thereby suggesting that ROS induced ER stress triggers several apoptotic signals including disturbances in MMP and Calcium homeostasis (fig.13) DNA fragmentation is regarded as late apoptosis parameters and requires incubation periods of 24 hours. Other markers defining apoptosis; especially MMP and caspase activation occur much earlier.

IV. CONCLUSION

The ZnSe/CdSe QDs exhibited maximum toxicity against Hep 3B cells, whereas, CdS/CdSe were moderately toxic at the tested doses Mainly, the cytotoxic effect of QDs can be due to heavy metal ions making up their composition that are capable of generating reactive oxygen species (ROS); nonspecific interaction with biological molecules. It can be proposed that initially, cadmium ions and selenium ions possibly get liberated from the shell of both the QDs causing cytotoxic effects by increased ROS generation in cancer cells which are already under continued ROS insult. The cellular uptake studies demonstrated that QDs-exposed cells at higher doses became abnormal in size, displaying cellular shrinkage, and an acquisition of an irregular shape. We report that QDs treatment induced ROS generation, possibly by causing ER stress induced enhanced release of intracellular calcium in the cytoplasm that further induced the depolarisation of MMP leading to release of mitochondrial cytochrome c into the cytoplasm. Release of cytochrome c causes induction of caspase-dependent cascade pathway. Cytochrome c cleaves pro-caspase-9 into its active form that subsequently activates effector caspase-3 and eventually triggered apoptosis of Hep3B cells suggested by the fragmented DNA**.** These results suggested that cytotoxicity of QDs in Hep3B cells followed the apoptotic pathway primarily mediated through oxidative stress induced ER stress mediated and mitochondrial mediated induction of caspase cascade pathway. These findings suggest that QDs can be exploited as potential anti-cancer drugs.

ACKNOWLEDGMENT

AT is thankful to UGC for her JRF. AL and NK are thankful to DBT for their respective JRF& SRF. DM acknowledges UGC for her SRF. This work was done without any financial assistance.

REFERENCES

[1] El-Serag H.B., Rudolph K.L. (2007) Hepatocellular carcinoma:epidemiology and molecular carcinogenesis. Gastroenterology, 132:2557-2576.

[2] Bruchez, M., Moronne, M., Gin, P., Weiss, S., Alivisatos, A.P. (1998). Semiconductor nanocrystals as fluorescent biological labels. Science, 281: 2013-2016.

[3] Taton, T., Mirkin, C., Letsinger, R. (2000) Scanometric DNA array detection with nanoparticle probes. Science, 289: 1757–1760.

[4] Cui, Y., Wei, Q., Park, H., Lieber, C. (2001). Nanowire nanosensors for highly sensitive and selective detection of biological and chemical species. Science, 293: 1289–1292.

[5] Chen, T., Zhao, T., Wei, D., Wei, Y., Li, Y., and Zhang, H. (2013). Core–shell nanocarriers with ZnO quantum dots-conjugated Au nanoparticle for tumor-targeted drug delivery. Carbohydrate polymers, 92(2): 1124-1132.

[6] Matea, C.T., Mocan, T., Tabaran, F., Pop, T., Mosteanu, O., Puia, C. and Mocan, L. (2017). Quantum dots in imaging, drug delivery and sensor applications. International journal of nanomedicine, 12:5421.

[7] Xiong, H. M., Xu, Y., Ren, Q. G., and Xia, Y. Y. (2008). Stable aqueous ZnO@polymer core–shell nanoparticles with tunable photoluminescence and their application in cell imaging. J. Am. Chem. Soc., 130(24):7522-7523

[8] Sanwlani, S., Rawat, K., Pal, M., Bohidar, H. B., and Verma, A. K. (2014). Cellular uptake induced biotoxicity of surface-modified CdSe quantum dots. Journal of Nanoparticle Research, 16(5): 23-82.

[9] Bhanoth, S., More, P., Jadhav, A. and Khanna, P.K. (2014) Core-Shell ZnSe-CdSe Quantum Dots: A Facile Approach via Decomposition of Cyclohexeno-1,2,3-Selenadiazole. RSC Advances, 4: 17526-17532.

[10] Bhanoth S., Kshirsagar A., Khanna P.K., Tyagi A., Leekha A., Kumar V. and Verma A.K. (2016a) Synthesis, Characterization and Bio-Evaluation of Core-Shell QDs with ZnSe, CdS and CdSe combinations. Adv. Mater. Lett., 7(12): 100-150.

[11] Bhanoth S., Kshirsagar A., Khanna P.K., Tyagi A., Verma A.K. (2016b) Biotoxicity of CdS/CdSe Core-Shell Nano-Structures. Advances in Nanoparticles, 5: 1-8.

[12] Bhanoth S., Tyagi A., Verma A.K. and Khanna P.K. (2016c) Cytotoxicity studies of II-VI semiconductor quantum dots on various cancer cell lines. Advanced Materials Letters, 8 (1):432-438.

[13] Yamakawa S., Demizu A., Kawaratani Y., Nagaoka Y., Terada Y., Maruyama S. and Uesato S. (2008) Growth inhibition of human colon cancer cell line HCT116 by bis(2-(acylamino)phenyl) disulfide and its action mechanism. Biological & Pharmaceutical Bulletin , 31(5): 916-920.

[14] Habig W.H., Pabst M.J. and Jakoby W.B. (1974) Glutathione S-transferases. The first enzymatic step in mercapturic acid formation. J Biol Chem., 249(22):7130-9

[15] Maria S. Moron, Joseph W. Depierre, Bengt Mannervik (1979) Levels of glutathione, glutathione reductase and glutathione S-transferase activities in rat lung and liver. Biochimica et Biophysica Acta, 582(1):67-78

[16] Bertoncini C.R., Meneghini R. (1995) DNA strand breaks produced by oxidative stress in mammalian cells exhibit 3'-phosphoglycolate termini. Nucleic Acids Res., 23(15):2995-3002.

[17] Roberts, J.A. and Hubel, C.A. (2004) Is oxidative stress the link in the two-stage model of preeclampsia? Lancet, 354:788-789.

[18] Fulda, S., Galluzzi, L., Kroemer, G. (2010) Targeting mitochondria for cancer therapy. Nat. Rev.Drug Discov., 9, 447–464.

[19] Pourahmad, J., O'Brien, P.J., Jokar, F., and Daraei, B. (2003). Carcinogenic metal induced sites of reactive oxygen species formation in hepatocytes. Toxicol. In Vitro., 17: 803-810.

[20] Andersson B.S., Aw, T. Y., Jones, D.P. (1987). Mitochondrial transmembrane potential and pH gradient during anoxia. Am J Physiol, 252 (4): 349-355.

[21] Tyagi A., Agarwal S., Leekha A. and Verma A.K. (2014). Effect of Mass and Aspect Heterogeneity of Chitosan Nanoparticles on Bactericidal Activity. International Journal of Advanced Research, 2(8): 357-367.

[22] Jani P., Halbert G.W., Langridge J., Florence A.T. (1990) Nanoparticle uptake by the rat gastrointestinal mucosa: quantitation and particle size dependency. J. Pharm. Pharmacol., 42: 821–826.

[23] Jimenez P.C., Wilke D.V., Takeara R., Lotufo T.M., Pessoa C. et al. (2008) Cytotoxicity activity of a dichloromethane extract and fractions obtained from Eudistoma vannamei (Tunicata: Ascidiacea). Comp Biochem Physiol A Mol Integr Physiol., 151: 391-398.

[24] Eruslanov E., Kusmartsev S. (2010) Identification of ROS using oxidized DCFDA and flow-cytometry. Methods Mol Biol., 594: 57-72.

[25] Jinhwan K., Tae Gyu C., Yan D., Yeonghwan K., Kwon S.H., Kyung Ho Lee, Insug K., Joohun Ha, Randal J. K., Jinhwa L., Wonchae C., and Sung Soo K. (2008) Overexpressed cyclophilin B suppresses apoptosis associated with ROS and Ca^{2+} homeostasis after ER stress. J Cell Sci., 1(121): 3636–3648.

[26] Moin I., Biswas L., Mittal D., Leekha A., Kumari N., Verma A.K. (2018) Crosstalk of ER Stress, Mitochondrial Membrane Potential and ROS Determines Cell Death Mechanisms Induced by Etoposide Loaded Gelatin Nanoparticles in MCF-7 Breast Cancer Cells. J Nanomed Nanotechnol., 9(4): 513.

[27] Verfaillie T., Garg A.D., Agostinis P. (2013) Targeting ER stress induced apoptosis and inflammation in cancer. Cancer Lett., 332: 249-264

[28] Hotokezaka Y., Van Leyen K., Lo EH.., Beatrix B., Katayama I., Jin G., Nakamura T. (2009) alphaNAC depletion as an initiator of ER stress-induced apoptosis in hypoxia. Cell Death Differ., 16:1505-1514

[29] He, N., Shi, X., Zhao, Y., Tian, L., Wang, D. (2013) Inhibitory effects and molecular mechanisms of selenium-containing tea polysaccharides on human breast cancer mcf-7 cells. J. Agric. Food Chem., 61:579–588.

[30] Bhandary B., Marahatta A., Kim H.R., Chae H.J. (2012) An involvement of oxidative stress in endoplasmic retimulum stress and its associated diseases. Int J Mol Sci., 14: 434-456.

[31] Kaltschmidt B., Kaltschmidt C., Hofmann T.G., Hehner S.P., Dröge W., Schmitz M.L. (2000) The pro- or anti-apoptotic function of NF-kappaB is determined by the nature of the apoptotic stimulus. Eur J Biochem., 267(12):3828-35.